Foam Rheology Near the Jamming Transition

Woldhuis, E.L.

Chapter 8

Testing the Non-linear Scaling Model

Now that we have fully derived the predictions for rheological behavior in our non-linear scaling method, we will test these predictions by direct simulation of a nonlinear particle model. The 'bubble model' code that we have used sofar (chapter 2), can not handle $\alpha_e \neq 1$, but does allow us to test $\alpha_v \neq 1$. Then in section 8.2.1 we will introduce a new code that, in principle, should be able to handle $\alpha_e \neq 1$. This new code is for particles of finite mass, allowing us to test the validity of our assumption of masslessness. To distinguish these two simulation codes we will call the one we have used until now the 'massless particle code' and the one that will be introduced in section 8.2.1 the massive particle code.

8.1 Massless Particle Code

With the massless particle code that we used throughout this thesis we have performed simulations of a wide range a different α_v's, including both $\alpha_v < 1$, $\alpha_v = 0.75$ and $\alpha_v = 0.5$, and $\alpha_v > 1$, $\alpha_v = 1.1$, $\alpha_v = 1.25$, $\alpha_v = 1.5$ and $\alpha_v = 2$. Unfortunately, we only have a limited sense of densities available for each α: 0.86, 0.85, 0.844 and in some cases 0.8424. We do have the full range of strain rate at our disposal, though.

In figure 8.1 we show collapse plots for the Transition and Critical regime for all six values of α, rescaled with the exponents given by table 7.1. While the data is preliminary, the results are consistent with our model predictions because we find collapse in all six plots onto power laws whose exponents are consistent with the predicted β's with the possible exceptions of the largest ($\alpha_v = 2$) and smallest ($\alpha_v = 0.5$) viscous exponents, see table 8.1. Two aspects of these plots are striking. First, the fact that for $\alpha_v < 1$, the highest strain-rate data falls below their power law curves. Second, the fact that

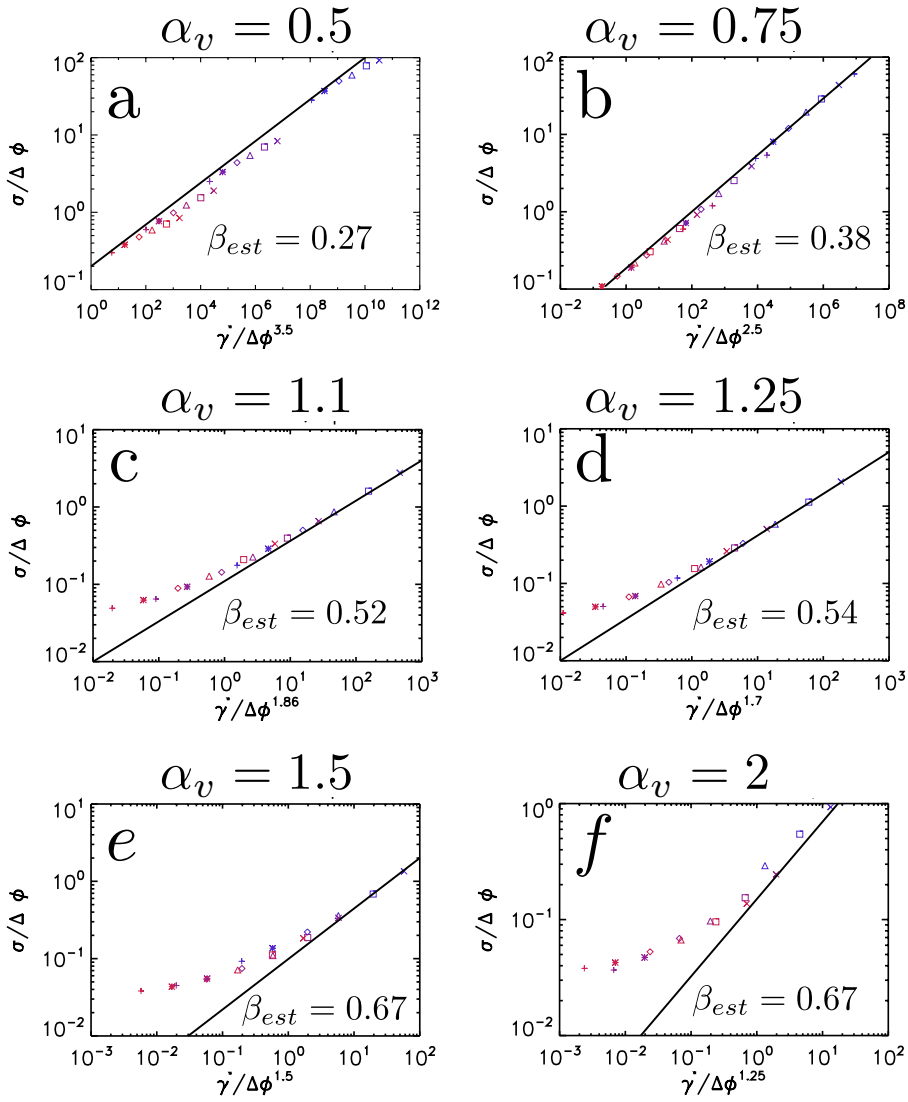

Figure 8.1: Transition and Critical regime collapse plots for **a** $\alpha_v = 0.5$, **b** $\alpha_v = 0.75$, **c** $\alpha_v = 1.1$, **d** $\alpha_v = 1.25$, **e** $\alpha_v = 1.5$ and **f** $\alpha_v = 2$. Symbols represent strain rates as in table 3.3. Colors represent density. From blue to red in **a** and **b**: 0.8424, 0.844, 0.85 and 0.86; and from blue to red in **c**, **d**, **e** and **f**: 0.844, 0.85 and 0.86. Black lines indicate best estimate power laws with exponent β_{est}, these values are consistent with our model predictions of table 8.1, except for $\alpha_v - 2$ - although the scaling range there is rather limited.

$\alpha_{\rm v}$	β_{est}	β_{model}
0.5	0.27	0.29
0.75	0.38	0.4
1.1	0.52	0.54
1.25	0.54	0.59
1.5	0.67	0.67
2	0.67	0.8

Table 8.1: Our estimate of β, β_{est}, for six different values of α compared to our model prediction, β_{model}.

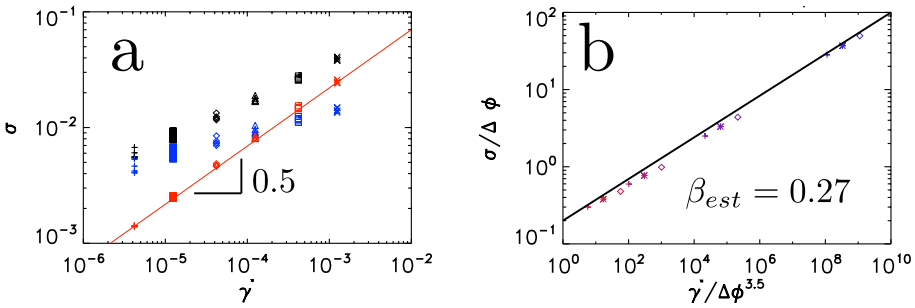

Figure 8.2: **a** Elastic (blue), viscous (red) and total (black) stress as a function of strain rate for $\alpha_{\rm v} = 0.5$. **b** Transition and Critical collapse plot for the slowest three strain rates of $\alpha = 0.5$. Colors represent density; from blue to red: 0.8424, 0.844, 0.85 and 0.86.

the Transition regime becomes more prominent for higher $\alpha_{\rm v}$. Both can be explained in the framework of our model.

First, the reason that high strain rate data falls below the curve in figures 8.1 **a** and **b** is that our strain rate criterion that $\dot{\gamma} < 10^{-2}$ for ensuring that the elastic stress dominates the viscous stress is no longer sufficient for $\alpha_{\rm v} < 1$. As we show in figure 8.2 **a**, for $\alpha_{\rm v} = 0.5$ the viscous stress, red, is larger than the elastic stress, blue, even for some strain rates that are smaller then 10^{-2}. This is in contrast to $\alpha_{\rm v} = 1$ where, as we have seen in figure 2.3, the elastic stress is significantly larger for all $\dot{\gamma} < 10^{-2}$. However, if we now plot only those strain rates for which the elastic stress *is* larger than the viscous stress, as we do in figure 8.2 **b**, we find that all data points now follow a single power law.

Second, since the crossover from the Transition to the Critical regime scales as $\dot{\gamma} \sim \Delta\phi^{(3+\alpha_{\rm v})/2\alpha_{\rm v}}$, this crossover shifts to higher strain rate as $\alpha_{\rm v}$ increases. Therefore, if data in the same density and strain rate range for different $\alpha_{\rm v}$

is compared, as it is in figure 8.1, more data will be in the Transition regime, and less data in the Critical regime for higher α_v. This is exactly what we see. Of course, since we rescale the horizontal $\dot{\gamma}$ axis with $\Delta\phi^{(3+\alpha_v)/2\alpha_v}$ to obtain collapse of this crossover, the crossover should always take place at the same value of $\dot{\gamma}/\Delta\phi^{\Gamma}$, and indeed if we compare the panels of figure 8.1, we see that the crossover always appears[1] at $\dot{\gamma}/\Delta\phi^{\Gamma} \approx 1$.

8.1.1 Conclusion

Our nonlinear scaling model predicts that the critical exponent β depends on the details of the (viscous) interaction. The data above, preliminary as it might be, corroborates this prediction, as shown in table 8.1. Even if the model would turn out to be not exact, it is clear that β *does* depend on α, and therefore the microscopic details of the interaction.

Our model does not make claims how changing the mode of dissipation to Mean Field [11, 27], inelastic collisions [29, 30] or thermostats [25, 28] might change the β, but since these changes are more far-reaching than simply changing the exponent of inter-particle viscous dissipation, we think it is unreasonable to assume that these changes will not impact β.

8.2 Massive Particle Code

The experimental and numerical results presented above have strengthened our belief that microscopic details are important for the rheology of soft particles near the jamming transition. Therefore we will investigate the effect of a non-zero mass in this section. In order to do this, we use a new simulation code developed jointly with Ellak Somfai. Below we will first introduce this new code that we will call the massive particle code, describing how it differs from the original massless particle code, and then discuss the findings that we have obtained using the code.

8.2.1 Implementation

Now that we have mass, and therefore acceleration, in our system, the first order forward Euler approach is no longer applicable. Therefore, the code is based on a second order 'velocity Verlet' algorithm. The algorithm works as follows:

- At time t we have $x(t)$, $v(t)$ and $a(t)$.
- We calculate the new position: $x(t+dt) = x(t) + v(t)dt + \frac{1}{2}a(t)dt^2$.
- We predict the new velocity: $\tilde{v} = v(t) + 0.65a(t)dt$; the value 0.65 can be changed, be have picked 0.65 because it was found to be optimal by [40].

[1] except for $\alpha_v = 0.5$, where all data points are to the right of $\dot{\gamma}/\Delta\phi^{\Gamma} \approx 1$

- We calculate the forces, $\tilde{F}$, based on $x(t+dt)$ and $\tilde{v}$, using the microscopic force expressions of Eqs. 7.1 and 7.2.
- We calculate the new acceleration: $a(t+dt) = \frac{\tilde{F}}{m}$.
- We calculate the actual new velocity: $v(t+dt) = v(t)+\frac{1}{2}[a(t)+a(t+dt)]dt$.
- Now we have x(t+dt), v(t+dt) and a(t+dt) and we can start the next iteration.

The mass of each particle is an adjustable parameter, meaning that we can, in principle, tune the importance of mass in the simulations. The unit of mass is chosen such that the density is 1, we label[2] this situation $m = 1$; in some cases we have also used particles with a masses that are ten times as big, denoted by $m = 10$, and 100 times as big, denoted by $m = 100$. An important caveat is that going to small mass will necessitate the use of very small time steps in order to prevent *overshoots* due to high acceleration. In practice this limits the range over which we can reduce the mass. Unless specified otherwise, the mass of each particle is proportional to its area (i.e. its two-dimensional volume) and set so that the density of the system is unity.

In addition, for a reason that we have not been able to determine, changing α_e away from 1, the linear case, requires going to very small time steps and causes crashes if the time step is too large. Unfortunately, this has made it impossible to study the effect of changing α_e away from 1 in our simulations.

8.2.2 Testing the Effect of Mass

We have performed a number of tests to see if the results of simulations with the new code make sense and in which regimes, if any, the effects of the presence of mass are strong and which regimes they are weak. We perform three tests: we have checked whether power balance is upheld is the new simulations, we have checked where the kinetic stress, that we use as a proxy for the presence of mass, is largest and we have directly compared the elastic stress in both the massless and massive particle codes.

Power Balance

Power balance is a fundamental concept and should hold in our system with mass also. The presence of mass does give a new way to temporarily store energy: in the form of kinetic energy. However, in steady state the amount of kinetic energy is constant (when averaged over long enough time scales). This

[2]This is indeed merely a label because the bidiserse particles have different masses and neither of them are 1; however we are not interested in the value of the mass, merely in the relative size of the mass between different simulations.

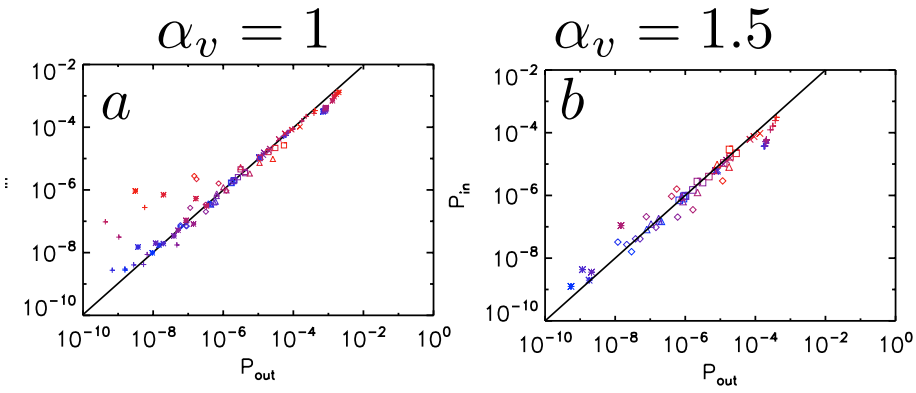

Figure 8.3: Power balance is upheld for $\alpha_{\mathrm{v}} = 1$ and $\alpha_{\mathrm{v}} = 1.5$

means there can be no net growth or decline of the kinetic energy and therefore the general expression for power balance that we introduced in Eq. 7.4:

$$\sigma_{xy}\dot{\gamma} \sim \Delta v^{1+\alpha_{\mathrm{v}}} \tag{8.1}$$

must hold. In figures 8.3 we show graphs testing power balance for two different α_{v}: $\alpha_{\mathrm{v}} = 1$ in panel **a** and $\alpha_{\mathrm{v}} = 3/2$ in panel **b**. As expected, power balance holds for both $\alpha_{\mathrm{v}} = 1$, the simple linear case, and $\alpha_{\mathrm{v}} = \frac{3}{2}$, giving an indication that these simulations are doing what they should do.

However, in figure 8.4 we show that for $\alpha_{\mathrm{v}} = \frac{1}{2}$, power balance breaks down for small strain rate, where the dissipated power appears to become larger than the input power. We hypothesise that this is a consequence of the concave shape of the microscopic viscous force for $\alpha_{\mathrm{v}} < 1$. In this case, a relatively small Δv already induces a relatively large force and there is a singularity at $\Delta v = 0$. To illustrate how this might lead to an overestimation of the dissipated power, consider the following example. Two bubbles, A and B, are moving in the same direction with velocities that are very similar, but A is slightly faster. These bubbles will exert viscous forces on each other that are comparatively large due to the square root viscous force law: A will pull B forward, B will drag A backwards. Thus, if the time step is not small enough, it may happen that the velocity adjustment that is a consequence of the viscous force will actually overshoot the 'intended' result of equal velocities: now B is faster than A. Instead of quickly reaching the same velocity, A and B keep rubbing past each other, dissipating large amounts of energy as they go. Such numerical problems may explain why the dissipated power is too large for small strain rates for $\alpha_{\mathrm{v}} < 1$.

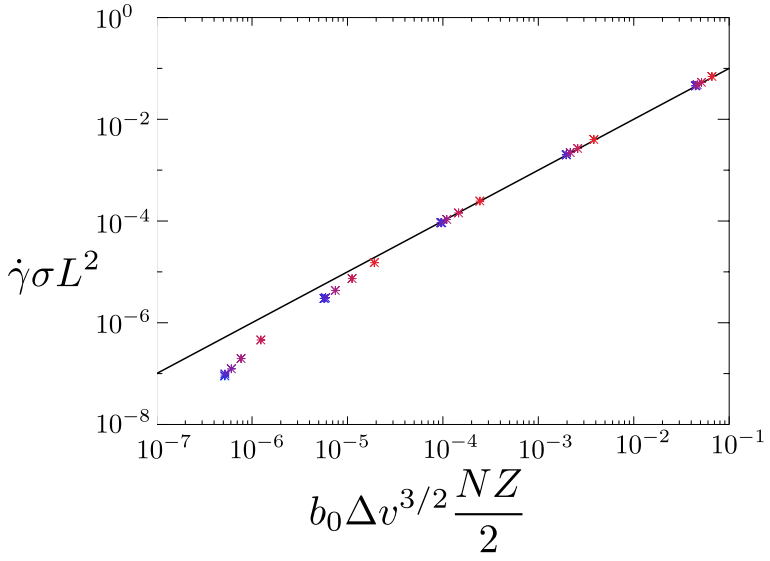

Figure 8.4: Power balance is not upheld for $\alpha_{\mathrm{v}} = 0.5$ for small strain rates.

Kinetic Stress

When elastic and viscous forces are not balanced, there is an extra contribution to the stress, called the kinetic stress, $\sigma^{xy}_{\mathrm{kin}} = m/2V \sum_{<ij>} v_{ij,x} v_{ij,y}$. In effect, the kinetic stress is the stress caused by the net forces on each particle. Clearly, if there is a sizeable kinetic stress relative to the elastic contribution to the stress[3], then mass plays an important role. We cannot strictly say that if the kinetic stress is small than the mass must have no effect. However, it is hard to imagine mass playing an important role in a system in which inertial effects are minimal, therefore we think that the ratio of the kinetic stress to the elastic stress is a good proxy for the effect of mass in our system.

Figure 8.5 shows the value of the kinetic stress as a fraction of the elastic stress. This fraction is plotted vs. the strain rate. In principle there should be graphs for all four components - xx, yy, xy, yx - but we have simply plotted the component for which the kinetic stress ratio is highest, the normal stress. Even in this case, though, the kinetic stress never passes beyond 1% of the elastic stress. The relative size of the kinetic stress is mostly determined by the strain rate - the higher the strain rate, the more important the kinetic stress - and is approximately linear in the strain rate for large densities. Hence, based on the relative magnitude of kinetic and elastic stresses, we would expect that the theologies of massive and massless particles would deviate most for high strain rates.

[3]Since, in our case, the elastic stress dominates, it is the relevant quantity to compare with.

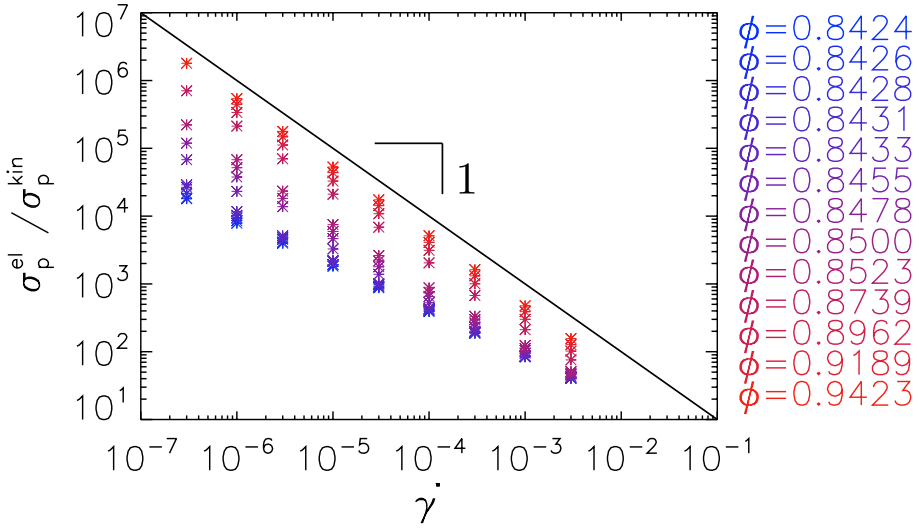

Figure 8.5: The kinetic stress as a fraction of the elastic stress as a function of strain rate for $m = 1$.

Direct Comparison

Instead of looking at whether the mass has an effect on the behavior at the system in general, we can directly check if it has an effect on the most important aspect of the system: the elastic stress. Figure 8.6 shows the elastic stress as a function of the strain rate (rescaled for collapse in the Transition and Yield regimes) for the massless particle code and three different values of the mass in the massive particle code: $m = 1$, $m = 10$ and $m = 100$. We immediately notice interesting behavior in the Yield stress regime: all three datasets with mass go to the same plateau, while the massless data does not go there. This is a strong indication that mass does not only play a role, but that the $m \downarrow 0$ limit might be singular. The behavior in the Critical regime is much more similar between mass and no mass and certainly seems more well behaved in the sense that the no-mass behavior seems to be the $m \downarrow 0$ limit of the data with a mass. What is surprising, considering the results for the kinetic stress ratio above, is that the most fundamental effect of mass is in the Yield regime. In this regime the strain rate is low and the density is high, exactly the opposite of where the kinetic stress ratio was highest.

In conclusion, it seems that the kinetic stress ratio is not a good predictor of how much the elastic stress will change due to the presence of mass. This is somewhat problematic because it means we do not have a way to judge the impact of mass in systems in which we can not compare to the massless case as we did for the $\alpha_e = \alpha_v = 1$ linear case above. One other parameter that we investigated is the distribution of Δv as this is another quantity where we

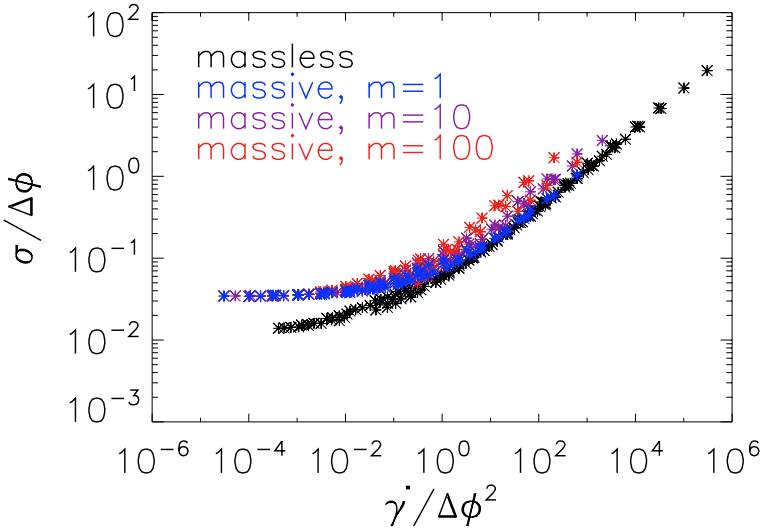

Figure 8.6: The elastic shear stress in simulations with different masses. There appears to be a fundamental difference between having any mass and having no mass at all.

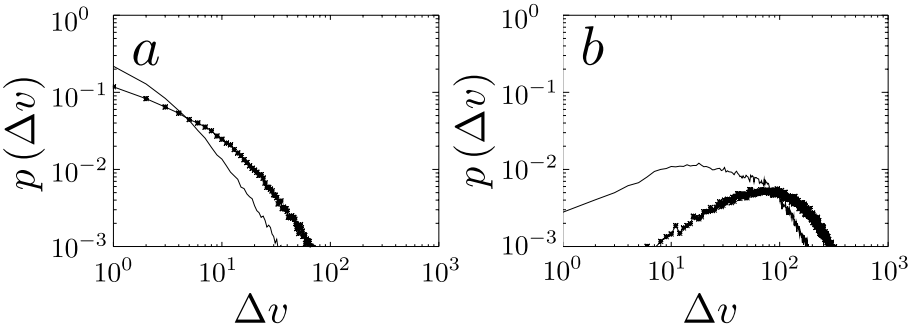

Figure 8.7: Comparison between the probability distribution functions of the relative velocity for the massless (line) and massive ($*$) particle codes for a system in the Critical regime (**a**: $\phi = 0.8424$, $\dot{\gamma} = 3 \cdot 10^{-3}$) and in the Yield regime (**b**: $\phi = 0.94$, $\dot{\gamma} = 10^{-5}$).

α_v	β
1.5	0.67
1.75	0.74
2	0.8
3	1

Table 8.2: Our model predictions β for the four different values of α that we investigate in this section.

expect the mass, through the acceleration, to have a large effect. As we show in figure 8.7 we do see that there is a large difference between $p(\Delta v)$ in the massless and massive particle codes in the Yield regime, while this difference is much smaller in the Critical regimes. This result agrees with our direct comparison of the elastic stresses: differences are large in the Yield regime and small(er) in the Critical regime.

8.2.3 Different α_v

Although the behavior of the elastic stress in the Critical regime does depend on the mass, for $\alpha_v = 1$ it does so in a well-behaved way: reducing the mass reduces the deviations from massless behavior. Therefore, it is possible to compare the exponent of the stress in the Critical regime, β, between our model predictions and massless simulations on the one hand and the massive simulations on the other hand if we pick a small mass and focus on the Critical regime. This we will do in the section below.

Since, as we have seen above, there are some numerical issues when picking an α_v below 1, we will focus on $\alpha_v > 1$, namely $\alpha_v = 1.5$, $\alpha_v = 1.75$, $\alpha_v = 2$ and $\alpha_v = 3$. Table 8.2 lists our model predictions β for the four different values of α that we investigate in this section.

Figure 8.8 shows a rescaled plot of stress vs. strain rate for $\alpha_v = 1.5$, $\alpha_v = 1.75$, $\alpha_v = 2$ and $\alpha_v = 3$. Panel **a**, $\alpha_v = 1.5$, shows clear collapse in the Critical regime, as we predict. Moreover, the Critical regime shows a $\frac{2}{3}$ power law; also as we predict. The behavior in the Yield plateau is not as we expect: we expect no collapse (we plot for collapse in the Transition and Critical regimes) but we do see strong collapse of most data points. As discussed above, we think this is a consequence of the fact that mass influences the Yield regime in a singular fashion. So far our model does well: it correctly predicts that what we expected it to predict: the Critical regime.

Collapse is slightly worse but for $\alpha_v = 1.75$, panel **b**, and much worse for $\alpha_v = 2$, panel **c**. It is clear that our model prediction completely break down for $\alpha_v = 3$, panel **d**. There are two possible explanations for the fact that the predictions of our model become worse as α_v increases. The first possible

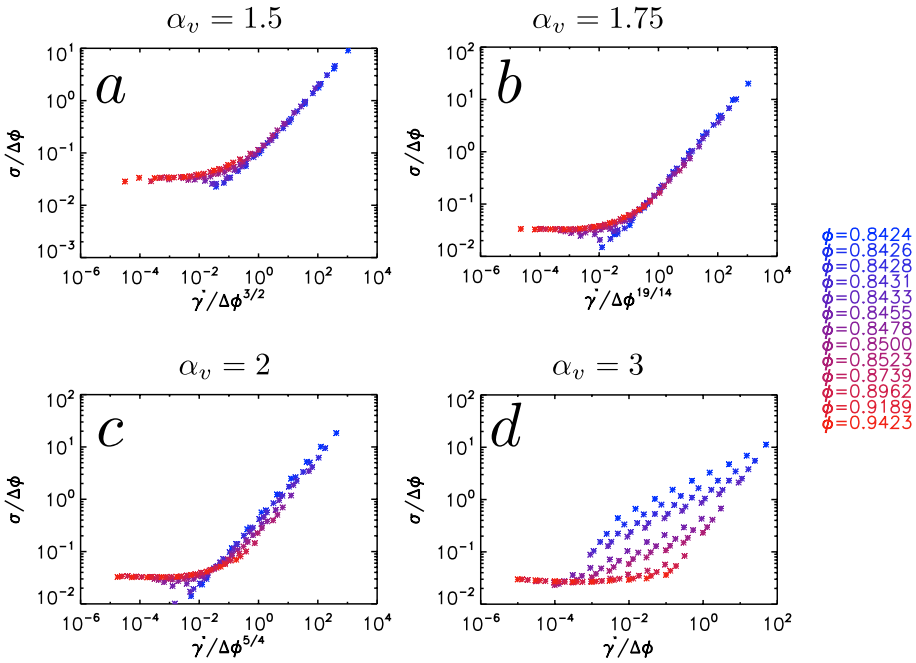

Figure 8.8: Elastic stress vs. the strain rate for $\alpha_{\rm v} = 1.5$, $\alpha_{\rm v} = 1.75$, $\alpha_{\rm v} = 2$ and $\alpha_{\rm v} = 3$, rescaled for collapse in the Transition and Critical regimes.

explanation is that some new physics enters for higher $\alpha_{\rm v}$ that our model fails to take into account properly. The second possible explanation is that at higher $\alpha_{\rm v}$, the mass has an increasing effect on that is necessary to avoid the effects of mass in the Critical regime, thus necessitating runs with $m = 0.1$ or smaller, which are numerically prohibitive..

8.3 Conclusion

We have tested the prediction of our model that β depends on the microscopic viscous interactions between our particles. We have tested this in two different simulation codes, one using massless particles and one using massive particles. The results from the massless particle simulations agree with our model for all investigated values of $\alpha_{\rm v}$. The picture is more complicated for the massive particle code: there are technical problems for $\alpha_{\rm v} < 1$ and for high $\alpha_{\rm v}$, 2 and 3, the model prediction does not agree with the simulation results. This may be a consequence of the fact that for various quantities adding mass to the simulations appears to be a singular perturbation.